Entrainment Threshold of Loose Boundary Streams

Subhasish Dey

1 Introduction

When a turbulent flow interacts with a loose boundary composed of noncohesive sediments, hydrodynamic forces are exerted on the sediment particles forming the boundary (henceforth bed). With an increase in flow velocity, the sediment particles on the bed surface are intermittently entrained at a random rate if the magnitude of the induced hydrodynamic forces acting on the sediment particles exceeds a certain threshold value. The condition that is just adequate to initiate sediment motion is termed *threshold* or *critical condition of sediment entrainment*. Importantly, the induced boundary shear stress of the stream flow in excess of that of the stream flow in threshold condition governs the sediment transport rate.

The doctoral research study by A.F. Shields (1936) on sediment movement conducted in the Technischen Hochschule Berlin was a phenomenal contribution (Kennedy 1995). His major finding was his diagram, well known as Shields diagram, that represents the variation of nondimensional threshold boundary shear stress (or threshold Shields parameter) with shear Reynolds number corresponding to the threshold of sediment entrainment. It is considered to be the reference of any sediment transport research. His pioneering work which is widely applied to the fields has inspired numerous researchers conducting further studies. However, not many attempts were made before Shields (1936), but they were mostly empirical with limited applicability. Despite the fact that the Shields diagram is widely applied, even as of today, researchers have expressed some dissatisfactions (Mantz 1977; Miller et al. 1977; Yalin and Karahan 1979; Buffington 1999), since the diagram less complies with the experimental data plots in the smooth and rough-flow regimes (Yalin and Karahan 1979). Thus, further attempts have so far been made to modify the Shields diagram, conducting additional experiments and analyzing the problem theoretically based on deterministic

S. Dey
Department of Civil Engineering, Indian Institute of Technology, Kharagpur, West Bengal 721302, India
e-mail: sdey@iitkgp.ac.in

P. Rowinski (ed.), *Experimental Methods in Hydraulic Research*,
Geoplanet: Earth and Planetary Sciences, DOI 10.1007/978-3-642-17475-9_2,

and probabilistic approaches. Miller et al. (1977), Buffington and Montgomery (1997), Paphitis (2001), and Dey and Papanicolaou (2008) presented a survey on this topic. However, after the discovery of the bursting phenomenon in turbulent flows (Kline et al. 1967), it has created a new look to further explore the sediment entrainment problem. The turbulence is so far introduced as an average like Reynolds shear stress. The conditional statistics towards the bursting events can be the obvious treatment of the sediment entrainment problem, as the most important turbulent events remain implicit with an averaging process. Therefore, the merger of turbulence with a sediment entrainment theory demands its way in between a deterministic and a probabilistic approach. It leads to an open question that to what extent the micromechanical process can be studied in a deterministic framework and when the results can be determined by a probabilistic approach.

A brief perspective review of the important laboratory experimental and theoretical studies on entrainment threshold of sediments under steady stream flows is presented, highlighting the empirical formulations and semitheoretical analyses. Special attention is given towards the role of the turbulent bursting on sediment entrainment.

2 Definition of Entrainment Threshold of Sediments

It is always difficult to set a clear definition of the threshold of sediment entrainment. First type of definition corresponds to the sediment flux. Shields (1936) suggested that the boundary shear stress has a value for which the extrapolated sediment flux vanishes. On the other hand, USWES (1936) put forward that the tractive force is such that produces a *general motion* of bed particles. For the median diameter of sediment particles less than 0.6 mm, this concept was found to be invalid. Thus, the general motion was redefined that the sediment in motion should reasonably be represented by all sizes of bed particles, such that the sediment flux should be greater than 4.1×10^{-4} kg/sm. Paintal (1971) suggested from stochastic viewpoint that due to the fluctuating mode of the instantaneous velocity, there is no mean boundary shear stress below which there is no flux. With this consideration, the threshold condition was defined as the boundary shear stress that produces a certain minimal amount of sediment flux.

Second type of definition corresponds to the bed particle motion. Kramer (1935) defined four types of boundary shear stress conditions for which: (1) no particles are in motion, termed *no transport*; (2) a small number of smallest particles are in motion at isolated zones, termed *weak transport*; (3) many particles of mean size are in motion, termed *medium transport*; and (4) particles of all sizes are in motion at all points and at all times, termed *general transport*. However, Kramer (1935) expressed the difficulty in setting a clear demarcation between these regimes, but defined threshold boundary shear stress to be the stress that initiates a *general transport*. Vanoni (1964) proposed that the sediment threshold is the condition of particle motion in every 2 s at any location of a bed. Different threshold definitions

that were in use in various studies leading discrepancies in the data sets and introducing difficulties in making comparisons (Paintal 1971; Buffington and Montgomery 1997).

3 Competent Velocity Concept

A competent velocity is a velocity at the particle level (boundary velocity) or the depth-averaged velocity, which is just adequate to start the particle movement for a given size. Goncharov (1964) used the competent velocity as detachment velocity U_n. It was defined as the lowest average velocity at which individual particles continually detach from the bed. He gave an equation of U_n as:

$$U_n = \log(8.8h/d)(0.57\Delta gd)^{0.5} \tag{1}$$

where h = flow depth; d = representative particle diameter, that is median particle diameter; g = acceleration due to gravity; $\Delta = s - 1$; s = relative density of sediment, that is ρ_s/ρ; ρ_s = mass density of sediment; and ρ = mass density of fluid.

Carstens (1966) proposed an equation of competent velocity u_{cr} at the particle level by analyzing a large number of experimental data. It is:

$$u_{cr}^2/\Delta gd \approx 3.61(\tan\varphi\cos\theta - \sin\theta) \tag{2}$$

where φ = angle of repose of sediment; and θ = angle made by the streamwise sloping bed with the horizontal.

Neill (1968) proposed a design curve for the initial movement of coarse uniform gravels in terms of average-velocity U_{cr} as a competent velocity. It is:

$$U_{cr}^2/\Delta gd = 2(h/d)^{1/3} \tag{3}$$

The forces acting on a spherical sediment particle resting on the bed of an open channel were analyzed by Yang (1973) to propose the equations for both smooth and rough boundaries as follows:

$$\frac{U_{cr}}{w_{ss}} = \frac{2.5}{\log R_* - 0.06} + 0.66 \quad \text{for } 0 < R_* < 70 \tag{4a}$$

$$U_{cr}/w_{ss} = 2.05 \quad \text{for } R_* \geqslant 70 \tag{4b}$$

where w_{ss} = terminal fall velocity; R_* = shear Reynolds number, that is u_*d/υ; u_* = shear velocity; and υ = kinematic viscosity of fluid.

Zanke (1977) recommended the following equation:

$$U_{cr} = 2.8(\Delta gd)^{0.5} + 14.7c_1(\upsilon/d) \tag{5}$$

where c_1 = coefficient varying from 1 for noncohesive to 0.1 for cohesive sediments. Many researchers have categorically disapproved the concept of competent velocity. The unanswered question is as to what is meant by the competent velocity at particle level u_{cr} or the competent average-velocity U_{cr}. This confusion has insisted the researchers to seek a more acceptable standard quantity like the threshold boundary shear stress. Nevertheless, Yang's (1973) analysis for the estimation of U_{cr} seems to be reasonable.

4 Lift Force Concept

Einstein (1950), Velikanov (1955), Yalin (1963), Gessler (1966), and Ling (1995) thought that the sediment is entrained solely by the lift force. The lift force can primarily be induced for the following reasons: (1) Sediment particles on the bed surface experience maximum velocity gradient, and thus a lift acts on the particles due to considerable pressure difference; (2) sediment particles may experience lift due to the instantaneous vertical velocity fluctuations in the vicinity of the bed; and (3) the spinning motion of sediment particles may result in lift due to Magnus effect (Dey 1999). Note that if the lift force equals the submerged weight of the particle, then drag force is adequate to entrain the bed particles.

Jeffreys (1929) assumed a potential flow over a circular cylinder having its axis perpendicular to the flow arguing that the lift is prevalent if $(3 + \pi^2)U^2 > 9\Delta g r_1$, where r_1 = radius of the cylinder. To apply this result, modification factors should be accounted for, as the two-dimensional model behaves in a different way than a three-dimension spherical particle in a fluid flow. The drawback of the analysis was that the drag force was ignored. Reitz (1936) discussed a similar idea to express the sediment entrainment with a lift model, where circulation and viscosity were important parameters of his analysis. Lane and Kalinske (1939) emphasized on turbulence for the quantification of lift and assumed that (a) the particles experience lift when their terminal fall velocity is smaller than the instantaneous vertical velocity fluctuations in the vicinity of the bed, (b) the variation of velocity fluctuations follows a normal-error law, and (c) a correlation exists between the velocity fluctuations and shear velocities. Einstein and El-Samni (1949) measured the lift force directly as a pressure difference and proposed the lift force per unit area $f_L = 0.5 C_L \rho (u_{0.35d})^2$, where C_L = lift coefficient assumed as 0.178; and $u_{0.35d}$ = flow velocity at an elevation $0.35d$ from the theoretical bed. They also studied the turbulent fluctuations on the lift. The experiments revealed a constant average lift force with superimposed random fluctuations that follow the normal-error law. Their results were used by the Task Committee (1966) estimating $f_L/\tau_c \approx 2.5$; where τ_c = threshold boundary shear stress. It suggests that the lift force is an important mechanism of the threshold of sediment entrainment. However, Chepil (1961) pointed out that once the particle moves, the lift and drag tend to diminish and increase, respectively. Chepil (1961) measured that the lift to drag ratio is about 0.85 for $47 < UD/\upsilon < 5 \times 10^3$, in a wind stream on hemispherical roughness

having diameter D, while Brayshaw et al. (1983) measured the ratio as 1.8 for the same roughness at $R_* = 5.2 \times 10^4$. Aksoy (1973) and Bagnold (1974) found the lift to drag ratio on a sphere of about 0.1 and 0.5 at $R_* = 300$ and 800, respectively. Apperley (1968) studied a sphere laid on gravels and found lift to drag ratio as 0.5 at $R_* = 70$. Watters and Rao (1971) observed negative (downwards) lift force on a sphere for $20 < R_* < 100$. Davies and Samad (1978) also reported that the lift force on a sphere adjacent to the bed becomes negative if significant underflow takes place beneath the sphere and the flow condition is $R_* < 5$. However, the lift is positive for $R_* \geq 5$, although the negative lift force could not be clearly explained.

While the lift forces obviously contribute to the sediment entrainment, the occurrence of lift on a sediment particle is still unclear. Insufficient experimental results are available to determine quantitative relationships; as such a critical lift criterion has so far not been obtained which could have been a ready reference for the determination of sediment entrainment. The occurrence of negative lift at low R_* has been well established, but its cause and magnitude remain uncertain. It was understood that besides the lift, the drag is always prevalent to contribute towards the sediment entrainment. For higher R_*, the correlation between lift and drag is another uncertain issue, although the lift is definitely positive.

5 Threshold Shear Stress Concept

5.1 Empirical Equations of Threshold Shear Stress

Attempts have been made to correlate the threshold boundary shear stress τ_c with sediment properties for experimental and field data. Kramer (1935) proposed:

$$\tau_c = 29\sqrt{(\rho_s - \rho)gd/M} \tag{6}$$

where τ_c is in g/m^2; M is the uniformity coefficient of Kramer; and d is in mm. Equation (6) is applicable for $0.24 \leq d \leq 6.52$ mm and $0.265 \leq M \leq 1$.

USWES (1936) recommended the following formula:

$$\tau_c = 0.285\sqrt{\Delta d/M} \tag{7}$$

where τ_c is in Pa; and d is in mm. Equation (7) is valid for $0.205 \leq d \leq 4.077$ mm and $0.28 \leq M \leq 0.643$.

A simple equation of τ_c is given by Leliavsky (1966) as:

$$\tau_c = 166d \tag{8}$$

where τ_c is in g/m^2; and d is in mm. None of the equations take into account the effect of fluid viscosity. Further, each of these equations produces results that differ

from each other. However, the empirical equations estimate the approximate values of τ_c, and their use cannot be recommended for the precise estimations.

5.2 Semitheoretical Analyses

Shields (1936) was the pioneer to propose a semitheoretical theory for the entrainment threshold of sediments. The threshold of particle motion is governed by balancing the driving force (as drag force) and the stabilizing resistance. At the threshold condition, when the sediment particle is about to move, $u_* \rightarrow u_{*c}$ (i.e., the threshold shear velocity) that has led to the following functional representation:

$$\Theta_c = f(R_*) \tag{9}$$

where Θ_c = threshold Shields parameter, ${u_{*c}}^2/\Delta g d$ or $\tau_c/\Delta\rho g d$. Figure 1 that shows the Shields' experimental results, which relate Θ_c and R_*, is known as *Shields diagram*. Figure 1 depicts three distinct flow zones: (1) Smooth flow for $R_* \leq 2$: in this case, d is much smaller than the thickness of viscous sublayer, and it is linearly varying that $\Theta_c = 0.1/R_*$. (2) Rough flow for $R_* \geq 500$: the viscous sublayer does not exist. The threshold Shields parameter Θ_c is invariant of the fluid viscosity and has a constant value of 0.056. (3) Transitional flow for $2 \leq R_* \leq 500$: sediment particles are of the order of the thickness of viscous sublayer. There is a minimum value of $\Theta_c = 0.032$ corresponding to $R_* = 10$.

The shortcoming of the Shields diagram is that the viscous parameter does not have any effect for $R_* \geq 70$, but Θ_c still varies with R_* in this range. Furthermore, the τ_c and u_{*c} that are interchangeable are shown as dependent and independent

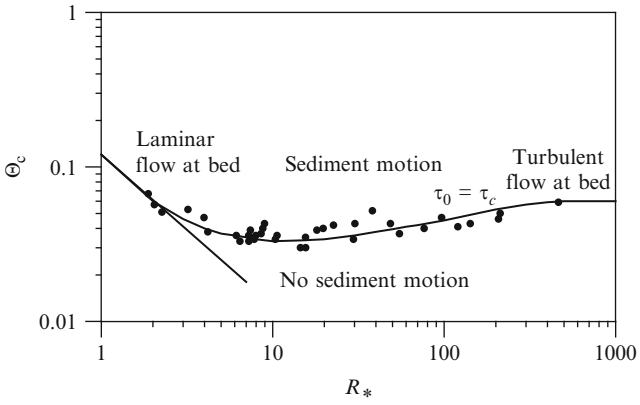

Fig. 1 Shields parameter Θ_c as a function of R_*

Table 1 Explicit empirical equations for the Shields diagram

Researchers	Equation
Brownlie (1981)	$\Theta_c = 0.22R_b^{-0.6} + 0.06\exp(-17.77R_b^{-0.6})$ where $R_d = d(\Delta g d)^{0.5}/\upsilon$
van Rijn (1984)	$\Theta_c(D_* \leqslant 4) = 0.24/D_*$ $\Theta_c(4 < D_* \leqslant 10) = 0.14/D_*^{0.64}$ $\Theta_c(10 < D_* \leqslant 20) = 0.04/D_*^{0.1}$ $\Theta_c(20 < D_* \leqslant 150) = 0.013D_*^{0.29}$ $\Theta_c(D_* > 150) = 0.055$ where D_* = particle parameter, that is $d(\Delta g/\upsilon^2)^{1/3}$
Soulsby and Whitehouse (1997)	$\Theta_c = \frac{0.24}{D_*} + 0.055[1 - \exp(-0.02D_*)]$
Paphitis (2001)	$\Theta_c(10^{-2} < R_* < 10^4) = \frac{0.273}{1+1.2D_*} + 0.046[1 - 0.57\exp(-0.02D_*)]$ It is the mean curve of Paphitis (2001)

variables in the diagram. Consequently, τ_c or u_{*c} remains implicit. Thus, attempts are made to derive explicit equations for the Shields diagram (Table 1).

In another study, White (1940) classified a high-speed case ($R_* \geq 3.5$) and a low-speed case ($R_* < 3.5$). High flow velocity is capable of moving larger particles. Therefore, the drag due to skin friction is insignificant as compared to the drag due to pressure difference. The packing coefficient p_f was defined by Nd^2, where N is the number of particles per unit area. The shear drag per particle (i.e., τ_c/N) is $\tau_c d^2/p_f$. At the threshold condition, the shear drag equals the product of the submerged weight of the particle and the frictional coefficient tan φ. Introducing a factor, termed *turbulence factor* T_f, he obtained:

$$\Theta_c = \frac{\pi}{6} p_f T_f \tan\varphi \quad \text{for } R_* \geqslant 3.5 \tag{10}$$

He proposed $p_f = 0.4$ and $T_f = 4$ for fully developed turbulent flow. On the other hand, low flow velocity is capable of moving smaller particles. In this case, the drag due to pressure difference acting on the particle is insignificant as compared to the viscous force. However, the upper portion of the particle is exposed to the shear drag that acts above the center of gravity of the particle. This effect is taken into account introducing a coefficient α_f. He proposed:

$$\Theta_c = \frac{\pi}{6} p_f\ \alpha_f \tan\varphi \quad \text{for } R_* < 3.5 \tag{11}$$

He suggested $p_f\ \alpha_f = 0.34$ as an average value.

Kurihara (1948) extended the work of White (1940) obtaining an expression for T_f in terms of R_*, turbulence intensity and the probability of boundary shear stress increment. The theoretical equations were quite complex. So he proposed simpler empirical equations of threshold boundary shear stress as

$$\begin{aligned}\Theta_c(X_2 \leqslant 0.1) &= (0.047\log X_2 - 0.023)\beta_2\\ \Theta_c(0.1 < X_2 \leqslant 0.25) &= (0.01\log X_2 + 0.034)\beta_2\\ \Theta_c(X_2 > 0.25) &= (0.0517\log X_2 + 0.057)\beta_2\end{aligned} \tag{12}$$

where $X_2 \approx 4.67 \times 10^{-3}[\Delta g/(\upsilon^2\beta_2)]^{1/3}d$; and $\beta_2\ (0.265 \leq M \leq 1) = (M + 2)/(1 + 2M)$.

Egiazaroff (1965) gave yet another derivation for $\Theta_c(R_*)$. He assumed that the velocity at an elevation of $0.63d$ (above the bottom of particle) equals the fall velocity w_{ss} of particle. His equation is

$$\Theta_c = \frac{1.33}{C_D[a_r + 5.75\log(0.63)]} \tag{13}$$

where $a_r = 8.5$; and C_D = drag coefficient = 0.4 for large R_*. Both a_r and C_D increase for low R_*. His results do not correspond with the Shields diagram.

Mantz (1977) proposed the extended Shields diagram to obtain the condition of maximum stability (Fig. 2). Yalin and Karahan (1979) presented a curve of Θ_c versus R_*, using a large volume of data collected from literature (Fig. 2). Their curve is regarded as a superior curve to the commonly used Shields curve.

Cao et al. (2006) derived the explicit equation for the curve of Yalin and Karahan (1979). It is:

$$\begin{aligned}\Theta_c(R_d \leqslant 6.61) &= 0.1414/R_d^{0.23}\\ \Theta_c(6.61 < R_d \leqslant 282.84) &= \frac{[1 + (0.0223R_b)^{2.84}]^{0.35}}{3.09R_d^{0.68}}\\ \Theta_c(R_d \geqslant 282.84) &= 0.045\end{aligned} \tag{14}$$

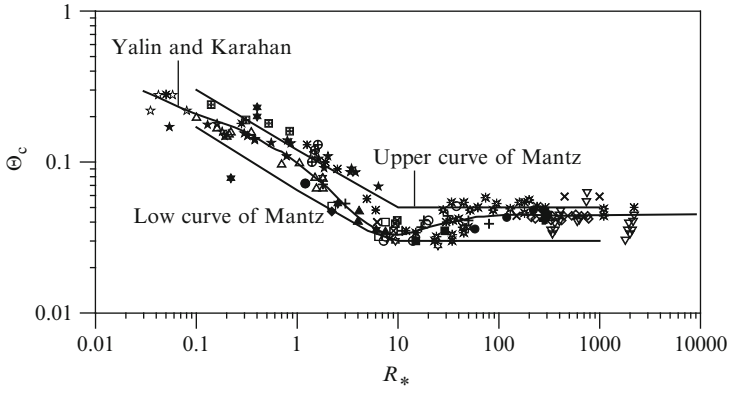

Fig. 2 Curves (Θ_c vs. R_*) of Mantz (1977) and Yalin and Karahan (1979)

Iwagaki (1956) analyzed the equilibrium of a single spherical particle, placed on a rough surface, and found the conditions necessary for the equilibrium of a particle in different conditions of viscous sublayer. The theoretical equation given by him is of the form:

$$\Theta_c = \frac{\tan\varphi}{\varepsilon_s \Psi_s R_*} \tag{15}$$

where ε_s = empirical coefficient for the sheltering effect; and Ψ_s = function of R_*.

The analysis of Ikeda (1982) that is based on Iwagaki (1956) and Coleman (1967) could approximately derive the Shields diagram. The analysis was based on forces acting on a solitary particle placed on a sediment bed. He obtained an equation as follows:

$$\Theta_c = \frac{4}{3}\cdot\frac{\tan\varphi}{(C_D + \tan\varphi C_L)}\cdot\left\{10.08R_*^{-10/3} + \left[\kappa^{-1}\ln\left(1+\frac{4.5R_*}{1+0.3R_*}\right)\right]^{-10/3}\right\}^{0.6} \tag{16}$$

where κ = von Kármán constant.

On a horizontal bed, the expression for the force balance given by Wiberg and Smith (1987) leads to:

$$\Theta_c = \frac{2}{C_D\alpha_0}\cdot\frac{1}{f^2(z/z_0)}\cdot\frac{\tan\varphi}{1+(F_L/F_D)_c\tan\varphi} \tag{17}$$

where $\alpha_0 = A_x d/V$; A_x = frontal area of the particle; V = volume of the particle; z = elevation from the bed; z_0 = zero-velocity level; $F_L/F_D = (C_L/C_D)f^2(z/z_0)/[f^2(z_T/z_0) - f^2(z_B/z_0)]$; z_T = elevation of the top point of the particle from the bed; and z_B = elevation of the bottom point of the particle from the bed.

Dey (1999) and Dey and Papanicolaou (2008) analyzed the hydrodynamic forces acting on a solitary particle resting over a horizontal sediment bed in a three-dimensional configuration (Fig. 3), including the effect of turbulent fluctuations.

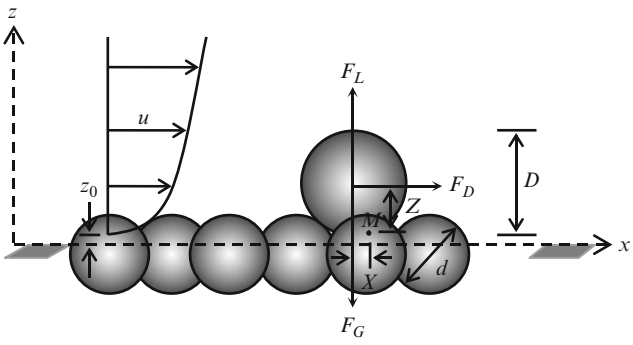

Fig. 3 Forces acting on a solitary particle in a three-dimensional configuration

Considering spherical particles, particle submerged weight $F_G = (\pi/6)\Delta\rho g D^3$ and hydrodynamic forces like drag $F_D = C_D(\pi/8)\rho u_m{}^2 D^2$ and lift (shear and Magnus lift) $F_L = C_L \rho u_m D^2(\partial u/\partial z)^{0.5}[\upsilon^{0.5} + 0.5f(R_*)D(\partial u/\partial z)^{0.5}]$ were taken into account. Here, D = diameter of solitary particle resting over a horizontal bed formed by the sediments of size d; u = flow velocity at elevation z; u_m = mean flow velocity received by the frontal area of solitary particle; $f(R_*) = 1$ for $R_* \geq 3$; and $f(R_*) = 0$ for $R_* < 3$. The lever-arms are $X = 0.433Dd/(D + d)$ and $Z = 0.289D(3D^2 + 6Dd - d^2)^{0.5}/(D + d)$. Taking moment at the pivot M, the equation for threshold condition was given by Dey as:

$$\Theta_c = \frac{2\pi\hat{d}/(1 + p\sqrt{\alpha - 1}\cos\psi)^2}{\pi C_D \hat{u}_m^2(3 + 6\hat{d} - \hat{d}^2)^{0.5} + 6C_L\hat{d}\hat{u}_m(\partial\hat{u}/\partial\hat{z})\{2[(R_*/\hat{d})\partial\hat{u}/\partial\hat{z}]^{-0.5} + f(R_*)\}} \tag{18}$$

where $\hat{d} = d/D$; $\hat{u} = u/u_{*c}$; $\hat{u}_m = u_m/u_{*c}$; $\hat{z} = z/D$; p = probability of occurring sweep event; ψ = sweep angle; $\alpha = \tau_t/\tau_c$; and τ_t = instantaneous shear stress. Using u for different flow regimes, Dey put forward a diagram for entrainment threshold as Θ_c versus D_* for different φ (Fig. 4). Unlike Shields diagram, it can be used directly for the determination of τ_c or u_{*c}.

Besides, James (1990) presented a generalized model of the threshold of sediment entrainment based on the analysis of forces acting on a particle, taking into account the particle geometry, packing arrangements and variations of near-bed flow velocity, drag, and lift. Ling (1995) studied the equilibrium of a solitary particle on a sediment bed, considering spinning motion of particles. He proposed two modes for limiting equilibrium, namely, rolling and lifting. McEwan and Heald (2001) analyzed the stability of randomly deposited bed particles using a discrete particle model. The threshold boundary shear stress could be adequately represented by a distribution of values. A Shields parameter of 0.06 for gravels found to correspond to the distribution for which 1.4% (by weight) of particles is on motion.

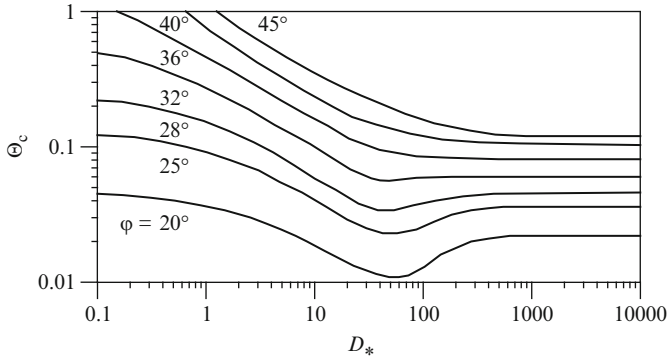

Fig. 4 Dependency of Θ_c on D_* for different φ

An analysis on sheltering of particles revealed that remote sheltering induced by the prominent upstream particles has an effect to increase the apparent threshold boundary shear stress of exposed particles.

6 Probabilistic Concept

The sediment entrainment is probabilistic in nature. It depends primarily on the turbulence characteristics in conjunction with the location of a specific particle relative to the surrounding particles of various sizes and their orientations. Gessler (1970) estimated the probability that particles of a specific size remain stationary. It was revealed that the probability of a given particle to remain stationary depends strongly on the Shields parameter and feebly on the shear Reynolds number. Grass (1970) proposed to use a probabilistic description of the stresses acting on a single particle to achieve motion. He identified two probability distributions: one for the boundary shear stress τ_w induced by the fluid and other for the boundary shear stress τ_{wc} required to put the particle in motion. When these two distributions start overlapping (Fig. 5), the particles that have the lowest threshold boundary shear stress start to move. The representative magnitudes of the probability distributions are their standard deviations being used to describe the distance of the two mean boundary shear stresses as $\bar{\tau}_{wc} - \bar{\tau}_w = n(\sigma_c - \sigma_\tau)$. He experimentally obtained the relationships as $\sigma_\tau = 0.4\bar{\tau}_w$ and $\sigma_c = 0.3\bar{\tau}_{wc}$, which leads to $\bar{\tau}_w = \bar{\tau}_{wc} \times (1 - 0.3n)/(1 + 0.4n)$. For $n = 0.625$, the result collapses with that of Shields.

Mingmin and Qiwei (1982), who developed a stochastic model, expressed the statistical parameters using the velocity of bottom flow and particle size. The probability of incipient motion, life distribution of stationary particles, number of distributions of particles in incipient motion, and intensity of incipient motion were derived. Wu and Chou (2003) studied the rolling and lifting probabilities for sediment entrainment by introducing the probabilistic features of the turbulent fluctuations and particle shape. These probabilities were linked to the two separate criteria for incipient motion to study the threshold entrainment probabilities.

The discovery of the turbulent bursting phenomena has encouraged the researchers in further studying the role of turbulence on sediment entrainment. In an attempt

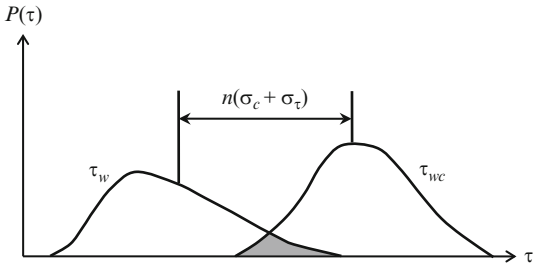

Fig. 5 Probabilities of boundary shear stress τ_w due to flow and threshold boundary shear stress τ_{wc} corresponding to the motion of individual particles

to link the characteristics of turbulent events with the threshold of sediment entrainment, Clifford et al. (1991) and Nelson et al. (1995) suggested that the Reynolds stress component is not the most relevant component to the sediment entrainment. However, the quadrant analysis by Papanicolaou et al. (2001) showed that the ratio of the Reynolds stress to the turbulence intensity is smaller in the beds with low-density particles than the densely packed ones. Hence, sediment entrainment criterion based solely on time-averaged boundary shear stress may underpredict the transport, especially in low-density packing cases. Based on these, Papanicolaou et al. (2002) developed a stochastic sediment threshold model that considered the role of near-bed turbulent structures and bed micro-topography upon the initiation of unisized particle motion. The model was based on the hypothesis that the probability of occurrence of exceeding the minimum moment required to initiate rolling motion equals the probability of first displacement of a particle. The theoretical derivation was complemented by the experimental measurements of the probability and near-bed turbulence for different packing regimes. They found it reasonable to consider that on average (temporal and spatial) for a sufficient large number of data, the probability of the occurrence of intermittent turbulent events equals the sediment entrainment probability. In another attempt, Dancey et al. (2002) proposed a criterion, which might be interpreted as the probability of individual particle motion, considering the statistical nature of sediment motion in turbulent flow and the time-scale of flow. The sediment threshold was specified by a constant value of the probability. However, a threshold criterion based upon the probability of particle motion could yield relatively active sediment beds, where the mechanism is strongly dependent upon the sediment packing density.

7 Role of Turbulence on Threshold of Sediment Entrainment

Cao (1997) proposed a model for the sediment entrainment based on the characteristics of the bursting structures (with time and spatial scaling) that are inherent in wall turbulent flows. He argued that the sediment entrainment is strongly dependent on the shear velocity. In another attempt, Zanke (2003) developed a model for the sediment threshold considering the influence of turbulence. He recognized two important effects as (a) the effective boundary shear stress acting on a particle increases above the time-averaged boundary shear stress owing to turbulent stress peaks and (b) the particles exposed to the flow become effectively lighter due to lift forces. Both the turbulence induced effects are randomly distributed. Dey and Raikar (2007) measured and analyzed the vertical distributions of time-averaged velocity and turbulence intensities in the flow on the near-threshold gravel beds. In the inner-layer, the law of the wall for the time-averaged velocity holds with $\kappa = 0.35$ and a constant of integration 7.8; while in the outer-layer, the law of the wake defines the velocity profiles with an average value of the Coles' wake parameter as 0.11. Nikora and Goring (2000) also observed the reduction of κ-value from its traditional value (0.41) in flows on a mobile gravel bed.

7.1 Turbulent Bursting

Experimental evidences on the viscous sublayer by Kline et al. (1967), Corino and Brodkey (1969), and Grass (1971) revealed a viscous dominating flow characteristic that consists of large three-dimensional high- and low-speed fluid steaks. The near-bed flow has an extremely complex structure producing large turbulence (Nezu and Nakagawa 1993). The emission of low-speed fluid streaks entraining to high-speed fluid streaks initiates the process of turbulent burst. The sequence turbulence bursting is described by two significant features as ejections and sweeps, which play an important role on entrainment of sediments. During the ejections, the upward flow enlarges the shear layer and the associated small-scale flow structures to a wide region. The ejection process is prevalent as low-speed fluid streaks that oscillate in three-dimension lifts up from the bed and then collapse to entrain into the main body of flow. The ejected fluid streaks which remain as a result of retardation are brushed away by high-speed fluid approaching to the bed in a process called the sweeps. During sweeps, the downward flow generates a narrow, highly turbulent shear layer containing multiple small-scale eddies. The turbulent bursting process and the contributions from the conditional Reynolds shear stress towards the total shear stress can be described by a quadrant analysis.

7.2 Quadrant Analysis

To understand the characteristics of the bursting events, it is necessary to study the conditional statistics of the velocity fluctuations (u' and w') plotting them to quadrants on a $u'w'$-plane (Lu and Willmarth 1973). A *hole-size* parameter H is used discriminating the larger contributions to $-\overline{u'w'}$ from each quadrant leaving the smaller u' and w' corresponding to more quiescent periods (Nezu and Nakagawa 1993). The curve $|u'w'| = H(\overline{u'u'})^{0.5}(\overline{w'w'})^{0.5}$ determines the hyperbolic hole region. In this way, a clear distinction is achieved between the strong and the weak events for a small hole-size and only strong events for a large hole-size. The types of bursting events are characterized by four quadrants i (= 1, 2, 3 and 4). They are (1) *outward interactions or* $Q1$ *events* ($i = 1$; $u' > 0, w' > 0$), (2) *ejections or* $Q2$ *events* ($i = 2$; $u' < 0, w' > 0$), (3) *inward interactions or* $Q3$ *events* ($i = 3$; $u' < 0, w' < 0$), and (4) *sweeps or* $Q4$ *events* ($i = 4$; $u' > 0, w' < 0$). The hole-size $H = 0$ implies that all data of u' and w' are taken into account. The quadrant analysis provides an estimation of the fractional contributions $S_{i,H}(= \langle u'w' \rangle_{i,H} / -\overline{u'w'})$ to $-\overline{u'w'}$ from the bursting events for quadrant i outside the hole region of size H. The contribution $\langle u'w' \rangle_{i,H}$ to $-\overline{u'w'}$ from the quadrant i outside the hole of size H is estimated by:

$$\langle u'w' \rangle_{i,H} = \lim_{T \to \infty} \frac{1}{T} \int_0^T u'(t)w'(t)\lambda_{i,H}(z,t)\mathrm{d}t \tag{19}$$

where T = time of sampling; and $\lambda_{i,H}(t)$ is the detection function given by $\lambda_{i,H}(t) = 1$, if (u', w') is in quadrant i and if $|u'w'| \geq H(\overline{u'u'})^{0.5}(w'w')^{0.5}$, and $\lambda_{i,H}(t) = 0$, otherwise. Here, $S_{i,H} > 0$ when $i = 2$ and 4 ($Q2$ and $Q4$ events), and $S_{i,H} < 0$ when $i = 1$ and 3 ($Q1$ and $Q3$ events). Hence, at a point, the algebraic summation of the contributions from different bursting events to $-\overline{u'w'}$ for $H = 0$ is unity, that is, $\sum_{i=0}^{i=4} S_{i,0} = 1$.

7.3 Earlier Developments

The role of turbulent bursting corresponding to the sediment entrainment seems to have received increasing attention. Sutherland (1967) observed that the sediment threshold is associated with a near-bed eddy impact onto the bed particles to produce a streamwise drag force that is large enough enabling to roll the particles. The role of the turbulent structures on the sediment entrainment was investigated by Heathershaw and Thorne (1985) in tidal channels. They argued that the entrainment is not correlated with the instantaneous Reynolds shear stress but correlated with the near-wall instantaneous streamwise velocity. Field observations by Drake et al. (1988) on mobility of gravels in alluvial streams suggested that the majority of the gravel entrainment is associated with the sweep events which give rise to the motion of particles. These events occur during a small fraction of time at any particular location of the bed. Thus, the entrainment process is rather episodic with short periods of high entrainment together with long periods of relatively feeble or no entrainment. Thorne et al. (1989) observed that sweeps and outward interactions play an important role in sediment entrainment. It is the instantaneous increase in streamwise velocity fluctuations that generate excess boundary shear stresses, governing entrainment processes. Having studied the sediment entrainment by nonuniform flows over two-dimensional dunes, Nelson et al. (1995) reported that the near-bed turbulence can change considerably and hence the sediment entrainment; while the boundary shear stress remains almost unchanged. They observed that when the magnitude of the outward interactions increases relative to the other bursting events, the sediment flux increases albeit the boundary shear stress decreases.

7.4 Recent Developments

Sarkar (2010) studied the turbulence characteristics on immobile and entrainment threshold sediment beds having uniform sediment size of 4.1 mm. A summary of the results obtained by him is furnished below:

In Fig. 6, the distributions of nondimensional Reynolds shear stress $-\overline{u'w'}/{u_*}^2$, as a function of nondimensional height z/h, are shown. Here, h is flow depth; and the solid line in Fig. 6 represents gravity line that follows $-\overline{u'w'}/{u_*}^2 = 1 - z/h$ for free surface flows having a zero-pressure gradient. Near the bed, the experimental distributions of Reynolds shear stress for immobile and entrainment threshold beds

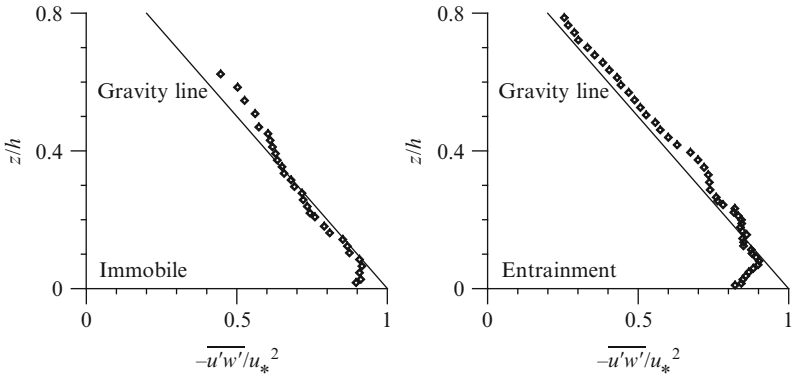

Fig. 6 Plots of $-\overline{u'w'}/u_*^2$ versus z/h for immobile and entrainment threshold beds

have a departure from the gravity line. On the other hand, in the upper flow zone, they are reasonably consistent with the gravity line, although they have a slight tendency to overestimate the gravity line. For $z/h < 0.1$ (near the bed), $-\overline{u'w'}/u_*^2$ for entrainment threshold beds diminishes more than that for immobile beds, although there is a general near-bed damping in the $-\overline{u'w'}$ due to roughness. The reduction in magnitude of $-\overline{u'w'}$ for entrainment threshold beds is attributed to the fact that a portion of the fluid turbulent stress is transferred to the bed particles to overcome the frictional resistance at the contacts of the entrained sediment particles. This is analogous to the concept of Grass (1970). The damping of the Reynolds shear stress can also be explained that the bed particles are associated with the provided momentum for the flow to maintain their motion.

Turbulent energy budget in two-dimensional flows is constituted by the turbulent production $t_P[= -\overline{u'w'}(\partial u/\partial z)]$ that is balanced by the summation of the turbulent dissipation ε, turbulent energy diffusion t_D $(= \partial f_{kw}/\partial z)$, pressure energy diffusion $p_D[= \partial(\overline{p'w'/\rho})/\partial z]$, and viscous diffusion v_D $[= -\upsilon(\partial^2 k/\partial z^2)]$; where $f_{kw} = 0.75(\overline{w'w'w'} + \overline{w'u'u'}$; p' = pressure fluctuations; and k = turbulent kinetic energy. In turbulent flows, the viscous diffusion v_D is insignificant. To evaluate ε, the relationship $\varepsilon = (15\upsilon/u^2)(\partial u'/\partial t)^2$ was used. The pressure energy diffusion p_D was estimated as $p_D = t_P - \varepsilon - t_D$. Figure 7a, b illustrates the energy budget in flows over immobile and entrainment threshold beds having uniform sediment size of 4.1 mm. The nondimensional form of these parameters are T_P, E_D, T_D, $P_D = (t_P, \varepsilon, t_D, p_D) \times (h/u_*^3)$. In general, T_P increases near the bed with an increase in z/h up to $z/h > 0.05$ and then decreases rapidly becoming nearly constant for $z/h > 0.3$. The distributions of E_D have a distinct lag from those of T_P. The influence of a sediment entrainment is apparent in the near-bed distributions of T_P and E_D, where the lag is reversed, which means $E_D > T_P$. Essentially, the difference of T_P and E_D at any depth is balanced by the combination of T_D and P_D. In Fig. 7a, b, T_D decreases with an increase in z/h within the wall-shear layer and then it becomes almost invariant of z/h. On the other hand, P_D attends a positive peak at $z/h \approx 0.05$ and then gradually decreases with an increase in

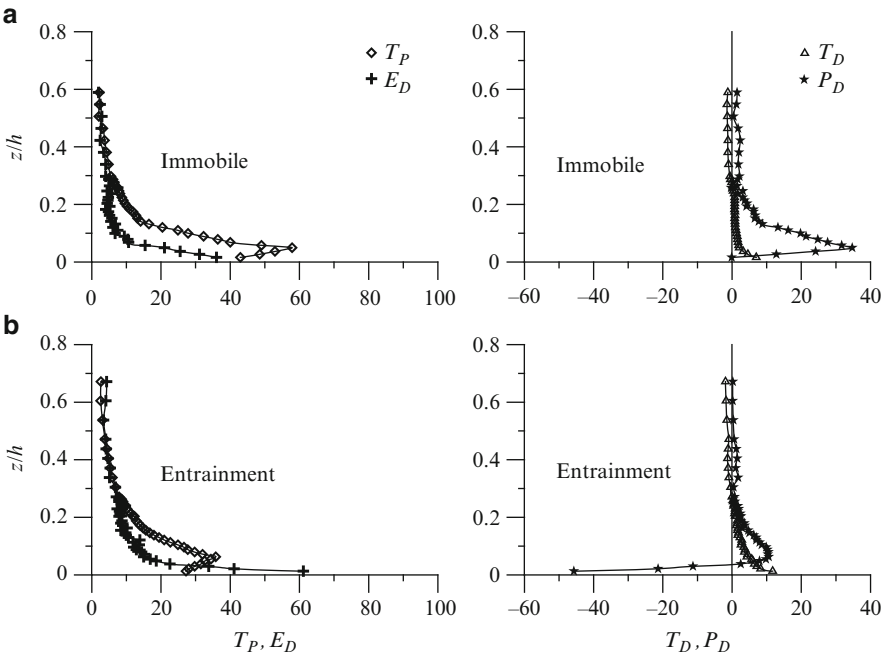

Fig. 7 Energy budget for (**a**) immobile and (**b**) entrainment threshold beds

z/h becoming a constant. The most interesting feature lies on the near-bed distributions of P_D in flows over entrainment threshold beds. It is apparent that the sediment entrainment is associated with a drastic changeover of P_D to a large negative value ($P_D \approx -45$). The negative value of P_D indicates a gain in turbulent production. It is therefore comprehensible that in near-bed flow zone over entrainment threshold beds, the turbulent dissipation exceeds the turbulent production and the pressure energy diffusion becomes considerably negative indicating a sediment entrainment.

The fractional contributions $S_{i,H}(z/h)$ towards the total Reynolds shear stress production from different bursting events, for the hole-sizes $H = 0$ and 2, are shown in Fig. 8a, b, respectively.

In Fig. 8a, for immobile beds, $Q2$ and $Q4$ events at the nearest point of the bed contribute about 75% ($S_{2,0} \approx S_{4,0} \approx 0.75$) to the total Reynolds shear stress production. On the other hand, $Q1$ events contribute moderately by 40% ($S_{1,0} \approx 0.4$), while $Q3$ events contribute minimal ($S_{3,0} \approx 0.1$). To be explicit, the arrival of low-speed fluid streaks from the near-bed region is revoked by the arrival of high-speed fluid streaks from the upper region. Thus, only a faster moving process is prevalent in the form of outward interactions $Q1$. In contrast, for entrainment threshold beds, $Q4$ events are the main mechanism to entrain sediments contributing about 90% ($S_{4,0} \approx 0.9$) towards the Reynolds shear stress production, while $Q2$ events contribute relatively less ($S_{2,0} \approx 0.6$). The tendency of $Q4$ events to dominate momentum transfer over a sediment bed is therefore strongly dependent upon the motion of surface particles.

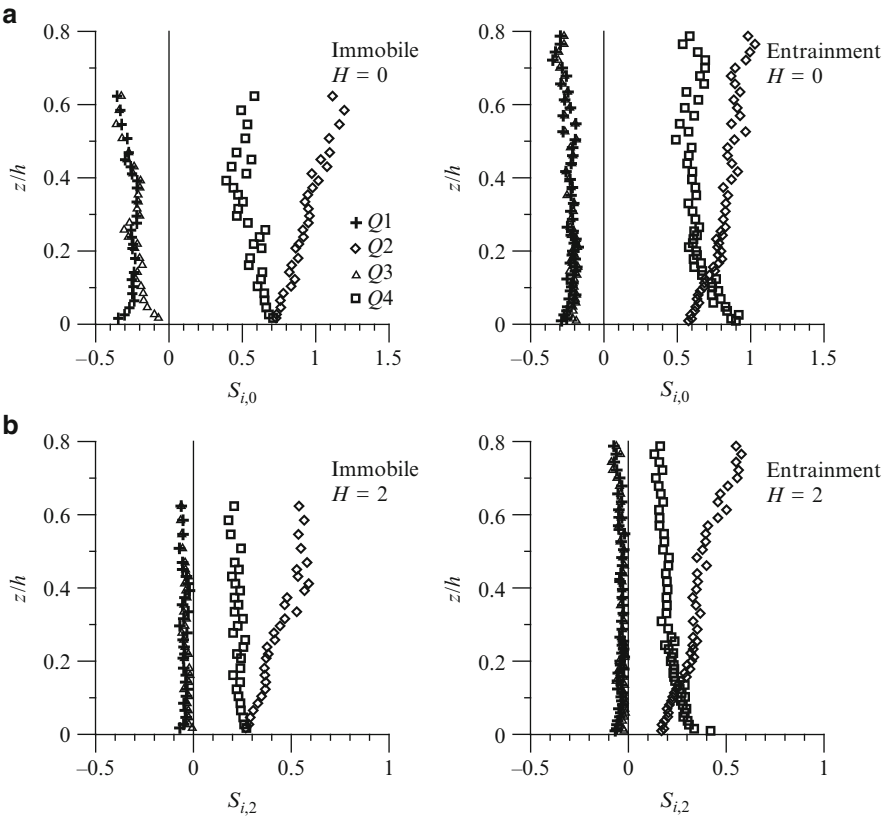

Fig. 8 Distributions of (**a**) $S_{i,0}(z/h)$ and (**b**) $S_{i,2}(z/h)$

It means the sediment motion is governed by the arrival of high-speed fluid streaks. But the contributions from $Q1$ and $Q3$ events are feeble ($S_{1,0} \approx 0.3$ and $S_{3,0} \approx 0.2$). Examining the Reynolds shear stress contributions from more extreme events occurring for hole-size $H = 2$ given in Fig. 8b, there remains a consensus that similar characteristics of most energetic $Q2$ and $Q4$ events prevail in the flow zone. Therefore, the quadrant analysis reveals that in the near-bed flow, ejections and sweeps in immobile beds rescind each other giving rise to the outward interactions, while sweeps are the dominant mechanism towards the sediment entrainment.

8 Closure

While plenty of researches have been carried out on the entrainment threshold of different sizes of sediments and all the investigations bring us a step nearer to an improved understanding of the sediment entrainment phenomenon in relation to the turbulence characteristics, there remains an inadequate attention to many cases.

For instance, the clear-cut role of turbulent coherent structure on sediment threshold is yet to be fully understood. Although there were some attempts, the flow fields were captured at least a couple of millimeters above the bed particles. Thus, the exact interaction between the particles and the fluid, in the level of particle micro-mechanics in association with the probabilistic feature of turbulence eddies, has not been completely revealed. Also, not many researchers have tried to explore the threshold of sediment entrainment for water worked beds. It is believed that the sediment threshold for water worked beds is different from those of manmade beds. Moreover, sediment threshold under the sheet flows or shallow flow depths seems to remain unattended. Therefore, further studies are required on these cases.

References

Aksoy S (1973) Fluid forces acting on a sphere near a solid boundary. In: Proceedings of 15th IAHR Congress, vol 1. Istanbul, Turkey, pp 217–224

Apperley LW (1968) Effect of turbulence on sediment entrainment. Ph.D. thesis, University of Auckland, New Zealand

Bagnold RA (1974) Fluid forces on a body in shear flow; experimental use of stationary flow. Proc R Soc Lond 340A:147–171

Brayshaw AC, Frostick LE, Reid I (1983) The hydrodynamics of particle clusters and sediment entrainment in course alluvial channels. Sedimentology 30:137–143

Brownlie WR (1981) Prediction of flow depth and sediment discharge in open channels. Report Number KH-R-43A, Keck Laboratory of Hydraulics and Water Resources, California Institute of Technology, Pasadena, California

Buffington JM (1999) The legend of A. F. Shields. J Hydraul Eng 125:376–387

Buffington JM, Montgomery DR (1997) A systematic analysis of eight decades of incipient motion studies, with special reference to gravel-bedded rivers. Water Resour Res 33:1993–2029

Cao Z (1997) Turbulent bursting-based sediment entrainment function. J Hydraul Eng 123:233–236

Cao Z, Pender G, Meng J (2006) Explicit formulation of the Shields diagram for incipient motion of sediment. J Hydraul Eng 132:1097–1099

Carstens MR (1966) An analytical and experimental study of bed ripples under water waves. Georgia Institute of Technology, School of Civil Engineering, Atlanta, Quarter reports 8 and 9

Chepil WS (1961) The use of spheres to measure lift and drag on wind-eroded soil grains. Proc Soil Sci Soc Am 25:343–345

Clifford NJ, McClatchey J, French JR (1991) Measurements of turbulence in the benthic boundary layer over a gravel bed and comparison between acoustic measurements and predictions of the bedload transport of marine gravels. Sedimentology 38:161–171

Coleman NL (1967) A theoretical and experimental study of drag and lift forces acting on a sphere resting on a hypothetical stream bed. Proceedings of 12th IAHR Congress, vol 3. Fort Collins, pp 185–192

Committee T (1966) Sediment transportation mechanics: initiation of motion. J Hydraul Div 92:291–314

Corino ER, Brodkey RS (1969) A visual investigation of the wall region in turbulent flow. J Fluid Mech 37:1–30

Dancey CL, Diplas P, Papanicolaou A, Bala M (2002) Probability of individual grain movement and threshold condition. J Hydraul Eng 128:1069–1075

Davies TRH, Samad MFA (1978) Fluid dynamic lift on a bed particle. J Hydraul Div 104:1171–1182

Dey S (1999) Sediment threshold. Appl Math Model 23:399–417

Dey S, Papanicolaou A (2008) Sediment threshold under stream flow: a state-of-the-art review. KSCE J Civ Eng 12:45–60
Dey S, Raikar RV (2007) Characteristics of loose rough boundary streams at near-threshold. J Hydraul Eng 133:288–304
Drake TG, Shreve RL, Dietrich WE, Whiting PJ, Leopold LB (1988) Bedload transport of fine gravel observed by motion picture photography. J Fluid Mech 192:193–217
Egiazaroff JV (1965) Calculation of non-uniform sediment concentrations. J Hydraul Div 91:225–247
Einstein HA (1950) The bed-load function for sediment transportation in open channel flows. US Department of Agriculture, Washington DC, Technical bulletin number 1026
Einstein HA, El-Samni EA (1949) Hydrodynamic forces on rough wall. Rev Mod Phys 21:520–524
Gessler J (1966) Geschiebetrieb bei mischungen untersucht an naturlichen, abpflasterungserscheinungen in kanalen. Nr. 69, Mitteilungen der Versuchsanstalt für Wasserbau und Erdbau, ETH Zurich, Germany
Gessler J (1970) Self-stabilizing tendencies of alluvial channels. J Waterway Harbors Div 96:235–249
Goncharov VN (1964) Dynamics of channel flow. Israel Programme for Scientific Translation, Moscow, Russia
Grass AJ (1970) Initial instability of fine bed sand. J Hydraul Div 96:619–632
Grass AJ (1971) Structural features of turbulent flow over smooth and rough boundaries. J Fluid Mech 50:233–255
Heathershaw AD, Thorne PD (1985) Sea-bed noises reveal role of turbulent bursting phenomenon in sediment transport by tidal currents. Nature 316:339–342
Ikeda S (1982) Incipient motion of sand particles on side slopes. J Hydraul Div 108:95–114
Iwagaki Y (1956) Fundamental study on critical tractive force. Trans JSCE 41:1–21
James C (1990) Prediction of entrainment conditions for nonuniform, noncohesive sediments. J Hydraul Res 28:25–41
Jeffreys H (1929) On the transport of sediments in stream. Proc Cambridge Philos Soc 25:272
Kennedy JF (1995) The Albert Shields story. J Hydraul Eng 121:766–772
Kline SJ, Reynolds WC, Straub FA, Runstadler PW (1967) The structure of turbulent boundary layers. J Fluid Mech 30:741–773
Kramer H (1935) Sand mixtures and sand movement in fluvial levels. Trans ASCE 100:798–838
Kurihara M (1948) On the critical tractive force, vol 4. Research Institute for Hydraulic Engineering, Report number 3
Lane EW, Kalinske AA (1939) The relation of suspended to bed materials in river. Trans Am Geophys Union 20:637
Leliavsky S (1966) An introduction to fluvial hydraulics. Dover, New York
Ling CH (1995) Criteria for incipient motion of spherical sediment particles. J Hydraul Eng 121:472–478
Lu SS, Willmarth WW (1973) Measurements of the structures of the Reynolds stress in a turbulent boundary layer. J Fluid Mech 60:481–571
Mantz PA (1977) Incipient transport of fine grains and flanks by fluids-extended Shields diagram. J Hydraul Div 103:601–615
McEwan I, Heald J (2001) Discrete particle modeling of entrainment from flat uniformly sized sediment beds. J Hydraul Eng 127:588–597
Miller MC, McCave IN, Komar PD (1977) Threshold of sediment motion under unidirectional currents. Sedimentology 24:507–527
Mingmin H, Qiwei H (1982) Stochastic model of incipient sediment motion. J Hydraul Div 108:211–224
Neill CR (1968) Note on initial movement of coarse uniform bed-material. J Hydraul Res 6:173–176
Nelson J, Shreve RL, McLean SR, Drake TG (1995) Role of near-bed turbulence structure in bed load transport and bed form mechanics. Water Resour Res 31:2071–2086

Nezu I, Nakagawa H (1993) Turbulence in open-channel flows. Balkema, Rotterdam, the Netherlands
Nikora V, Goring D (2000) Flow turbulence over fixed and weakly mobile gravel beds. J Hydraul Eng 126:679–690
Paintal A (1971) Concept of critical shear stress in loose boundary open channels. J Hydraul Res 9:91–113
Papanicolaou A, Diplas P, Dancey C, Balakrishnan M (2001) Surface roughness effects in near-bed turbulence: implications to sediment entrainment. J Eng Mech 127:211–218
Papanicolaou AN, Diplas P, Evaggelopoulos N, Fotopoulos S (2002) Stochastic incipient motion criterion for spheres under various bed packing conditions. J Hydraul Eng 128:369–380
Paphitis D (2001) Sediment movement under unidirectional flows: an assessment of empirical threshold curves. Coastal Eng 43:227–245
Reitz W (1936) Uber geschiebebewegung. Wasserwirtschaft und Technik, pp 28–30
Sarkar S (2010) Turbulence in loose boundary streams. Ph.D. thesis, Indian Institute of Technology, Kharagpur, India
Shields AF (1936) Application of similarity principles and turbulence research to bed-load movement, vol 26. Mitteilungen der Preussischen Versuchsanstalt für Wasserbau und Schiffbau, Berlin, Germany, pp 5–24
Soulsby RL, Whitehouse RJS (1997) Threshold of sediment motion in coastal Environments. Proceedings of combined Australasian coastal engineering and port conference, Christchurch, New Zealand, pp 149–154
Sutherland AJ (1967) Proposed mechanism for sediment entrainment by turbulent flows. J Geophys Res 72:6183–6194
Thorne PD, Williams JJ, Heathershaw AD (1989) In situ acoustic measurements of marine gravel threshold and transport. Sedimentology 36:61–74
USWES (1936) Flume tests made to develop a synthetic sand which will not form ripples when used in movable bed models. United States Waterways Experiment Station, Vieksburg, Technical memorandum 99-1
van Rijn LC (1984) Sediment transport, part I: bed-load transport. J Hydraul Eng 110: 1431–1456
Vanoni VA (1964) Measurements of critical shear stress. California Institute of Technology, Pasadena, Report number KH-R-7
Velikanov MA (1955) Dynamics of alluvial stream, vol 2. State Publishing House of Theoretical and Technical Literature, Russia (in Russian)
Watters GZ, Rao MVP (1971) Hydrodynamic effects of seepage on bed particles. J Hydraul Div 97:421–439
White CM (1940) The equilibrium of grains on the bed of a stream. Philos Trans R Soc 174A:322–338
Wiberg PL, Smith JD (1987) Calculations of the critical shear stress for motion of uniform and heterogeneous sediments. Water Resour Res 23:1471–1480
Wu FC, Chou YJ (2003) Rolling and lifting probabilities for sediment entrainment. J Hydraul Eng 129:110–119
Yalin MS (1963) An expression of bed-load transportation. J Hydraul Div 89:221–250
Yalin MS, Karahan E (1979) Inception of sediment transport. J Hydraul Div 105:1433–1443
Yang CT (1973) Incipient motion and sediment transport. J Hydraul Div 99:1679–1704
Zanke UCE (1977) Neuer Ansatz zur Berechnung des Transportbeginns von Sedimenten unter Stromungseinfluss. Mitteilungen Des Franzius-Institut, Technical University Hannover, Germany, Heft 46
Zanke UCE (2003) On the influence of turbulence on the initiation of sediment motion. Int J Sediment Res 18:17–31

http://www.springer.com/978-3-642-17474-2

Experimental Methods in Hydraulic Research
M. Rowiński, P. (Ed.)
2011, XXII, 322 p., Hardcover
ISBN: 978-3-642-17474-2